ENHANCING PAYLOAD CAPACITY WITH DUAL-ARM MANIPULATION AND ADAPTABLE MECHANICAL INTELLIGENCE

A Thesis
Presented to
The Academic Faculty

By

Raymond Kim

In Partial Fulfillment
of the Requirements for the Degree
Master of Science in the
George W. Woodruff School of Mechanical Engineering

Georgia Institute of Technology
December 2020

ENHANCING PAYLOAD CAPACITY WITH DUAL-ARM MANIPULATION AND ADAPTABLE MECHANICAL INTELLIGENCE

Approved by:

Dr. A. Mazumdar, Advisor
School of Mechanical Engineering
Georgia Institute of Technology

Dr. K.M. Lee
School of Mechanical Engineering
Georgia Institute of Technology

Dr. A. Young
School of Mechanical Engineering
Georgia Institute of Technology

Dr. S. Balakirsky
Institute for Robotics and Intelligent Machines
Georgia Tech Research Institute

Date Approved: July 13, 2020

This work is dedicated to my lord and savior Jesus Christ, who is and always will be, my constant source of support and encouragement.

ACKNOWLEDGEMENTS

All praise, honor, and glory to my Lord Jesus Christ for His richest grace and mercy for the accomplishment of this thesis. Without His blessings, this achievement would not have been possible.

I wish to express my sincere appreciation to my advisors, Dr. Anirban Mazumdar and Dr. Stephen Balakirsky, who have the substance of geniuses: they convincingly guided and encouraged me to be professional and do the right thing even when the road got tough. Without their persistent help, the goal of this project would not have been realized.

I want to acknowledge the physical and technical contribution of my colleagues over at Georgia Tech Research Institute. I would like to thank Matthew Marcum, Konrad Ahlin, and Spencer Fishman for their contributions. Without their support, this project would have never reached its goal.

I would like to thank all the DART Lab members who have supported and helped me finish this project. I would like to thank Adam Foris, Samuel Lutes, Zachary Goddard, Aakash Bajpai, Kathryn Bruss, Bharat Kanwar, Kevin Choi, Samuel Deal, Joshua Fernandez, and Pooja Moolchandani. They kept me going and this work would not have been possible without their support.

Finally, my deepest gratitude to my parents for their constant prayers and unconditional love. Their confidence bolstered my own through the ebb and flow of this work.

Once again, my sincere thanks to all.

- *Raymond Kim*

TABLE OF CONTENTS

Acknowledgments iv

List of Figures vii

Summary xi

Chapter 1: Introduction and Background 1

1.1 Challenges of Manipulating Heavy Objects 1

1.2 Various Approaches to Cooperative Manipulation 2

1.3 Paper Structure 4

Chapter 2: Gripper Mechanism Design 5

2.1 Functional Requirements 5

2.2 Dual-Arm Whiffletree Gripper Design 6

2.3 Whiffletree Mechanism 7

2.4 Passive Joints for Position Deviations 9

2.5 Tool Changers for Autonomous Installation 9

2.6 Customizable Grasping Tools 10

Chapter 3: Controls 15

3.1 Control Strategy 15

Chapter 4: Performance Quantification 21

4.1 Mechanical Prototype 21

4.2 Experiments 22

Chapter 5: Results 28

Chapter 6: Conclusion 33

Appendix A: Tool Changer Control 36

Appendix B: Pneumatics for Grasping System 38

References 44

LIST OF FIGURES

1.1 Dual-arm whiffletree gripper distributing the load evenly during a $7kg$ lift for two UR5 manipulators. The maximum payload for each manipulator is $5kg$. 1) Manipulator 1, 2) Manipulator 2, 3) Dual-arm whiffletree gripper, 4) $7kg$ wooden box. 1

2.1 Annotated design of the dual-arm whiffletree gripper: 1) Tool changer, 2) 3 DOF passive joint, 3) I-beam linkage, 4) central pivot joint, 5) four pneumatic suction cups. 6

2.2 The central pivot point of the whiffletree system can be changed to distribute the load in a desirable manner. Figure 2.2(a) shows an equal distribution of the load through the whiffletree mechanism. The center pivot point is at the center. 8

2.3 Uneven load distribution can also be achieved by changing the location of the central pivot point. Figure 2.3(a) shows a 2 to 1 ratio of the load distribution. The center pivot point is one-third distance from the left manipulator. 8

2.4 Passive joint has 3 DOF (Figure 2.4(a)). Each degree of freedom adds an additional rotation about each principal axis (x, y, and z). Figures 2.4(b) and 2.4(c) show that the rotations about axes x and y are enabled by rotary shafts with up to 100 degrees of rotation. Figure 2.4(d) illustrates that full vertical rotation is enabled by the turntable. Slots on the I-beam linkage allow horizontal displacements from any oscillatory behavior of the manipulators (Figure 2.4(e)). 11

2.5 Tool changers can be implemented to allow ease of transition between different tasks. The master plate (left) and the tool plate (right) can be interfaced to join the manipulator and the gripper. 12

2.6 The grasping tool can be customized for desired application. For this work, pneumatic suction cups were chosen for an industrial application setting. . . 13

2.7 The electromagnetic gripper design can be used to lift various ferrous materials. 13

2.8 The Robotiq 2-finger parallel gripper can be installed on the center joint and controlled via the electric module on the tool changers. 14

3.1 Representation of processes that occur at each time instance of control and path planning. No inverse kinematics operation is required for trajectory planning and motion. 15

3.2 A single Cartesian coordinate frame was defined to plan the path of the two manipulators. The two end-effectors were prioritized to stay a fixed relative distance from each other using attractive forces (F_{att1}). Multiple desired goal positions were set in sequence in order to plan the path and attractive forces (F_{att2}, F_{att3}, ...) were used follow the desired trajectory. . . 17

4.1 Annotated view of the fully designed and machined prototype of the dual-arm whiffletree gripper: 1) passive joint, 2) Robotiq Force-Torque Sensor, 3) Master Plate, 4) Tool Plate, 5) I-beam linkage, 6) center joint, 7) pneumatic grippers. 21

4.2 Experimental setup using two 6 DOF UR5 manipulators. The manipulators were setup $1.3m$ apart from each other to lift and carry a $7kg$ load. 24

4.3 Phase 1: The two UR5 manipulators approach the tool stand on the steel table to install the tool changers. The locking mechanism of the tool changers is triggered electronically via relay shield. 25

4.4 Phase 2: The two UR5 manipulators approach the wooden crate to grasp using the dual-arm whiffletree gripper. The plot shown on the top right indicates the force exerted on the two end-effectors in the z-direction. . . . 25

4.5 Phase 2: The pneumatic suction cups are used to grasp the wooden crate and are triggered using pneumatic valves. The graph shows the force dropping initially when the suction cups are pressed down using the pneumatic suction cups. 26

4.6 Phase 2: The two UR5 manipulators carry the box to the nearby cart. The graph shows a relatively even distribution of forces. 26

4.7 Phase 3: The box is released on the cart. 27

4.8 Phase 3: The two UR5 manipulators return to home position. 27

5.1 The force applied to the end-effectors in the z-direction when carrying a $7kg$ load. The forces are distributed evenly across the two manipulators. . . 29

5.2 Force measurements of the two manipulators during the dual-arm manipulation task. The $17s$ mark indicate the grasping of the wooden box using pneumatic suction cups. The $35s$ mark indicate the placement of the wooden box on the cart. Note that the sensors start recording after the installation of tool changers. 30

5.3 The forces applied to the end-effectors in the x and y-direction when carrying a $7kg$ load. The forces are distributed evenly across the two manipulators. 31

5.4 Plot of the path trajectory taken by the two UR5 manipulators during the experiment. 32

A.1 The setup for the 4-channel relay shield with an Arduino Uno. 36

B.1 Pneumatics diagram for the vacuum gripper. 38

B.2 Numatics Air Particulate Regulator was used to control the pressure of compressed air. 39

B.3 Three solenoid valves were connected to the relay shield to control the tool changers and the vacuum gripper. 40

SUMMARY

Manipulating large and heavy objects is a crucial task in various robotic applications such as agriculture, search and rescue, service, and manufacturing. While modern manipulators have advanced considerably, they are limited by their net load capacity. This places a fundamental limit on the weight of loads that a single manipulator can move. For a case where a large load exceeds the capacity of a single manipulator, there are two potential solutions. First, the manipulator can be replaced with a larger one to increase the maximum payload. This can be time-consuming and expensive. Alternatively, two manipulators can be used collaboratively to share the load. This enables use of existing manipulators.

Cooperative manipulation with two arms has the potential to increase the net load capacity of the system. However, it is critical that proper load sharing takes place between the two arms. If this is not maintained, the load limits of one of the arms can be exceeded and lead to catastrophic failure. Ensuring load sharing can be a challenging controls and coordination problem. In this work, a method that utilizes mechanical intelligence in the form of a whiffletree is outlined.

A whiffletree is a mechanical device that allows distribution of load through the use of pivot points and linkages. Whiffletrees are used in a range of applications including bionic limbs, under-actuated fingers, horse-harnesses on carriages, and wind turbine tests. Typically, a whiffletree consists of a bar pivoted at or near the center, with force applied from one direction to the pivot and from the other direction to the tips. The points on the linkage act as pivot points, allowing positional displacements for any attached loads.

This method is used to design, fabricate, and assemble the dual-arm whiffletree gripper system that enables load sharing amongst two manipulators. The mechanical properties of the whiffletree allows load distribution without any force sensory feedback and enables robustness to positional displacements. As a result, the system is able to integrate a simplified, position-control based strategy. To allow ease of integration to existing robotic

systems, the overall design of this work is easily attachable/detachable with various types of customizable grippers using pneumatic tool changers.

Physical experiments were conducted to illustrate the enhanced load capacity of a robotic system using the dual-arm whiffletree gripper. Specifically, two UR5 manipulators, each with $5kg$ maximum payload, are utilized to re-position a $7kg$ load. This load would exceed the capacity of a single arm, and the experimental results show that the forces on each arm remain below this level and are evenly distributed.

CHAPTER 1

INTRODUCTION AND BACKGROUND

1.1 Challenges of Manipulating Heavy Objects

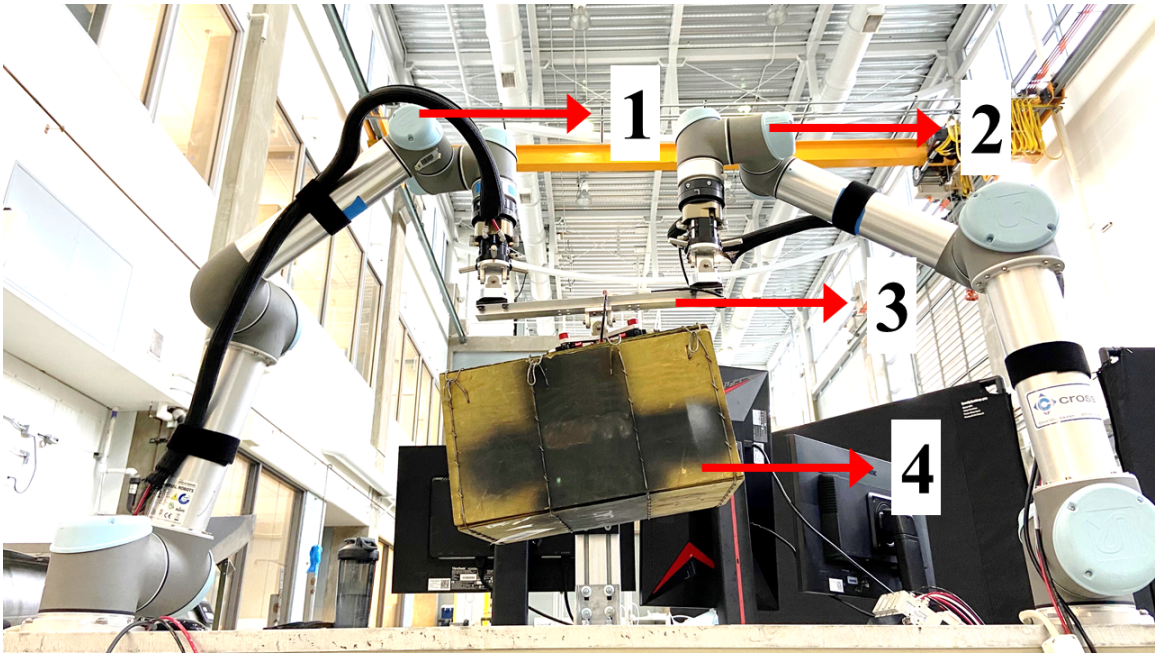

Figure 1.1: Dual-arm whiffletree gripper distributing the load evenly during a $7kg$ lift for two UR5 manipulators. The maximum payload for each manipulator is $5kg$. 1) Manipulator 1, 2) Manipulator 2, 3) Dual-arm whiffletree gripper, 4) $7kg$ wooden box.

Manipulation of large and heavy objects is important for numerous robotic application domains such as agriculture, manufacturing, search and rescue, and service robotics [1]. While modern manipulators have advanced considerably, they are still limited by the force and torque capacity of their actuators. For a case in which a large load exceeds the capacity of a single manipulator, there are two potential solutions. First, the manipulator can be replaced with a larger one. This can be time-consuming and expensive. Alternatively, two manipulators can work together to share the load. This enables use of existing manipulators.

Previous studies have highlighted how two manipulators working together can be used to handle flexible objects, share bulky or unwieldy payloads, or perform complex manipulation behaviors [2, 3]. However, increasing payload through sharing creates different challenges. The fundamental challenge when lifting excessive loads is load distribution. If a single manipulator carries the majority portion of the load, the robot will fail as a result of exceeding the payload capacity. Furthermore, if this problem is not addressed carefully, highly undesirable consequences may result, such as reduced life span of robot components, damaged parts, or task failure.

This work presents a new approach to dual-arm cooperative manipulation. The core contributions of this work are: 1) designing a whiffletree gripper intended specifically for autonomous robot manipulators, 2) describing how position-based control can be used in concert with the whiffletree mechanism for cooperative manipulation, 3) experimentally illustrating how load balancing can be achieved with a simplified control strategy that does not sense forces or attempt to balance them. To date, this work is the first to use the whiffletree mechanism to enable autonomous and adaptable load sharing between two robot manipulators.

1.2 Various Approaches to Cooperative Manipulation

Three different broad coordination strategies exist in the literature. The first method is the master-slave control scheme [4, 5]. In this control strategy, the master arm is instructed to follow a trajectory using position control, and the other is subject to compliant force control in order to maintain a kinematic constraint. The master-slave control strategy simplifies implementation by allowing each manipulator to have its own independent controller. However, this method does not attempt to distribute the load between the two arms. Recent studies that do consider the load distribution heavily rely on force sensors installed on the wrist of the manipulator [6, 7].

The second control strategy utilizes a centralized control architecture. In this method,

the manipulators and the grasped payload are considered a closed kinematic chain, based on a unified robot and payload dynamic model [8, 9]. Many studies determine the position and force constraints between the arms to implement force control [10–12]. Other studies show that the centralized control provides better coordination than the master-slave control scheme [13]. However, the implementation of a centralized controller can suffer from high computational load and a complicated architecture [14]. While computing and communication have been made easier with the advances in computing, the need to collect data from both robots creates failure modes and potential performance bottlenecks. Furthermore, certain centralized control methods require force sensors on the end-effectors, or actuators that can be force controlled in order to be implemented [15, 16].

The third control strategy is the decentralized control scheme. This involves controlling each manipulator with its own local controller with its own coordinate system [17, 18]. In comparison to the master-slave control scheme, there is no communication delay between the arms [14]. Compared to the centralized control scheme, the decentralized control scheme is much easier to implement. However, each manipulator must have a robust force feedback controller in order to maintain proper load distribution between manipulators [19]. As a result, this control scheme relies heavily on force-torque sensors or actuators that can be force controlled to control the interactions between the robots.

While effective, the aforementioned strategies suffer from some key drawbacks. Master-slave strategies rely on an effective compliance control strategy, which requires excellent sensing and actuation properties. Centralized control relies on effective communication. Decentralized control requires effective sensing and force control. In addition, independent controllers can cause excessive internal forces and unwanted oscillations. One of the most simple and effective solutions is to exploit mechanical properties such as structural flexibility. Compliant grippers with springs [20, 21], rubber tip installed fingers [22], and a pendulum-based gripper [23] are all examples that allow simplified control schemes.

The problem of load sharing has also been studied in the application of cranes. Nu-

merous patents use frames and mechanisms for adjustable load sharing amongst multiple cranes [24, 25]. These solutions use hoisting yokes or beams with cables to distribute the load uniformly over the points of suspension [26, 27].

1.3 Paper Structure

This work explores mechanically intelligent methods that can simplify coordination, sensing, and control. Specifically, a whiffletree is used to enable dual-robot manipulation with intrinsic load sharing capacity. This means that the load does not need to be balanced through sophisticated sensing and control. Instead, the mechanical system itself ensures that the loads on the two arms are balanced even when they move with different velocities. First, a set of functional requirements is outlined for this mechanically intelligent method. Then, the key components of the dual-arm whiffletree gripper design are illustrated and a functional mechanical prototype is presented. A position-based control strategy that can be used in concert with the whiffletree mechanism is described. This control strategy can be achieved without any force-feedback or sensors. Finally, results of the physical experiments are presented to illustrate the enhanced load capacity of an existing robotic system as shown in Figure 1.1. Specifically, two UR5 manipulators re-position a $7kg$ load. This load would exceed the capacity of a single arm, and the results show that the forces on each arm remain below the maximum payload and are relatively evenly distributed.

CHAPTER 2
GRIPPER MECHANISM DESIGN

2.1 Functional Requirements

This section describes the functional requirements for a system which enables two manipulators to carry loads beyond each manipulator's provided payload capacity. For the scope of this work, the focus is on 6 degree of freedom (DOF) industrial manipulators. However, these requirements are highly applicable to a broad range of manipulators. Specifically, the emphasis is on mechanical designs that enable position-based control, bearing of large loads, easy installation, and easy customization.

1. ***Distribution of load***: The primary aim of the mechanical device is to make sure the load is distributed during cooperative manipulation. If the load is not properly distributed, the load limits of one of the arms can be exceeded and lead to catastrophic failure.

2. ***Simplified control scheme***: The mechanical device should allow distribution of the load without any sensory or control feedback. The exclusion of sensors and complicated control schemes greatly simplifies the coordination between two manipulators.

3. ***Autonomous Installation***: The robot arms should be able to autonomously attach and detach from the mechanical device when needed. This prevents disruption to autonomous capabilities. To achieve this, the mechanical device should be capable of controllable attachment/detachment with low forces, and rapid turnaround.

4. ***Robustness to heavy loads***: The mechanical device must be able to withstand the loads without any damage, flexing, or failure.

5. ***Easy Customization***: The mechanical device should readily integrate to a range of robotic systems. This means that the mechanical device should be applicable to different types of manipulators, with various grasping methods.

A review of existing literature did not provide any readily available solution that met all of the listed functional requirements. Therefore, the approach adopted in this work presents a whiffletree mechanism that is specifically tailored for customized dual-arm manipulation. This system is described in detail in the following sections.

2.2 Dual-Arm Whiffletree Gripper Design

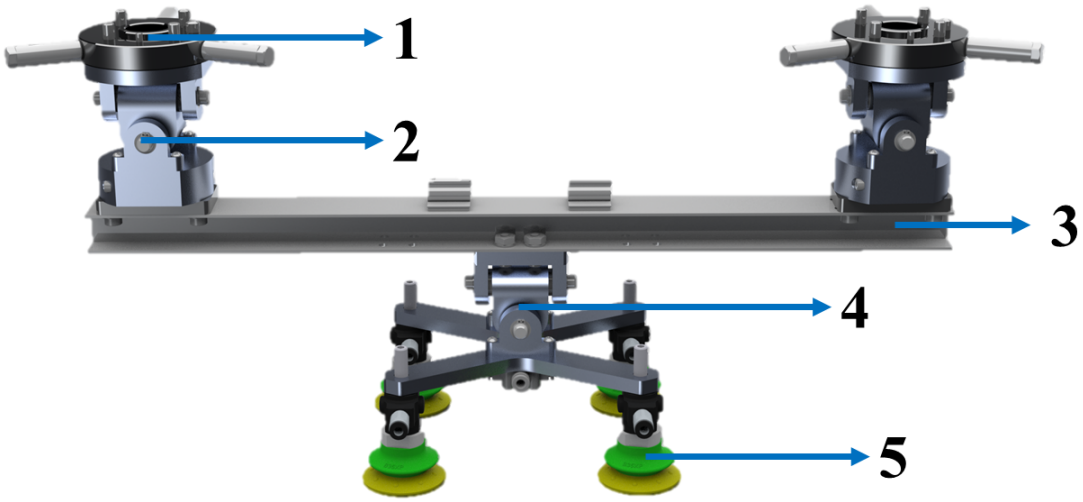

Figure 2.1: Annotated design of the dual-arm whiffletree gripper: 1) Tool changer, 2) 3 DOF passive joint, 3) I-beam linkage, 4) central pivot joint, 5) four pneumatic suction cups.

This section describes the overall design of the dual-arm whiffletree gripper, shown in Figure 2.1. The design utilizes a whiffletree mechanism to distribute the load amongst two manipulators. The gripper consists of two passive joints, a central pivot joint, and a linkage. The two passive joints are located at each tip of the linkage; each linked to a single manipulator. The central pivot point is located near the center of the linkage and is

extended to be a grasping device for the load. For this work, pneumatic suction cups were chosen to grasp heavy loads in an industrial setting. The linkage, which connects the two manipulators and the load, is designed to be an I-beam to maximize stiffness. Tool changers are attached to the ends of each passive joint to enable rapid, autonomous installations.

2.3 Whiffletree Mechanism

A whiffletree mechanism is a common load distributing mechanism used in various applications such as bionic limbs, under-actuated fingers, and wind turbine tests [28–30]. This mechanism consists of a bar pivoted at or near the center, with force applied from one direction to the pivot and from the other direction to the tips. The points on the linkage act as pivots allowing positional displacements for any attached loads.

Whiffletrees are typically used to allow even load distributions. For cases where uneven load distribution is preferred, the central pivot point can be relocated. Even load distributions are desired when two identical manipulators are used to lift a heavy load. Since many manipulators move relatively slowly, forces due to gravity often dominate. Therefore, this work is mainly interested in using the whiffletree to balance the forces in the earth-fixed (global) Z-axis. This enhances the Z-axis load capacity of the overall system. These benefits are restricted to the configurations where the whiffletree z-axis aligns with the earth-fixed Z-axis. For instance, Figure 2.2(a) shows a case where two identical UR5 manipulators, each with maximum payload of $5kg$, are used to lift a load. The central pivot point is placed equidistant from each other to allow equal distribution. For a given case where there are two different manipulators, a UR5 and a UR10, each with $5kg$ and $10kg$ maximum payloads respectively, the load must be distributed differently. The UR10 would need to carry a heavier portion of the weight due to its higher payload capacity. Static analysis can be done to calculate the placement of the central pivot point for any given scenario. Figure 2.2(b) and 2.3(b) show the load calculations through a static beam analysis. As long as the maximum payload of the manipulator is known, the location of the central

pivot point can be calculated for the correct load distribution. For the case with UR10 and a UR5, the UR10 must carry twice as much as the UR5. As shown in Figure 2.3(a), the central pivot point is one-third distant from UR10 and two-thirds distant from the UR5.

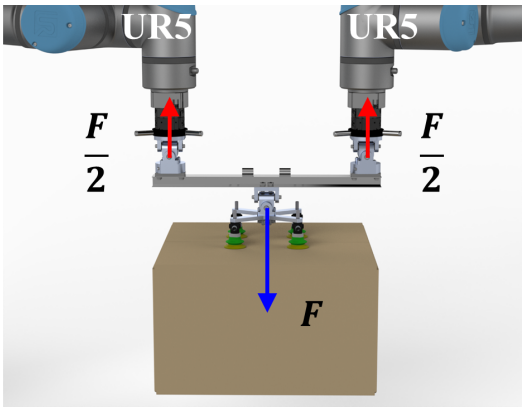

(a) Equal Load Distribution.

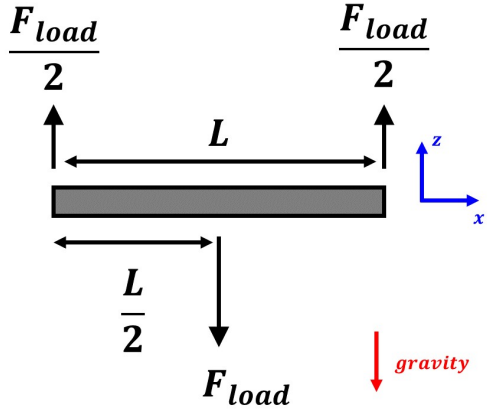

(b) FBD of equal distribution.

Figure 2.2: The central pivot point of the whiffletree system can be changed to distribute the load in a desirable manner. Figure 2.2(a) shows an equal distribution of the load through the whiffletree mechanism. The center pivot point is at the center.

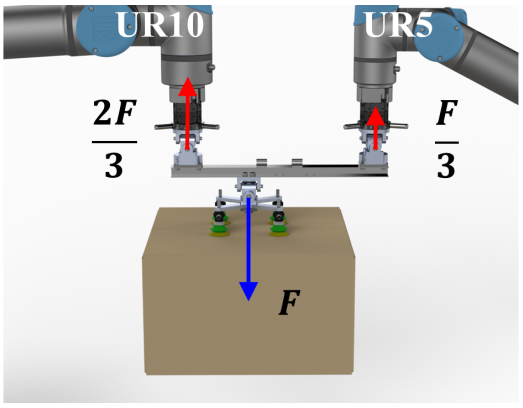

(a) 2 to 1 Load Distribution.

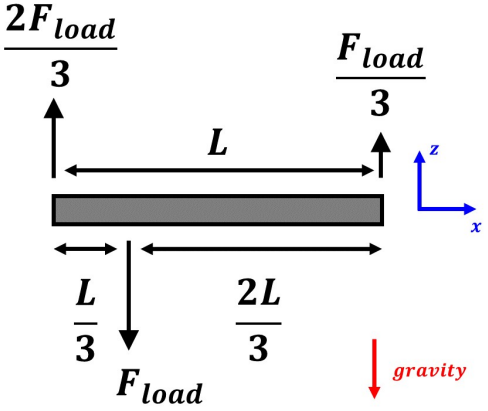

(b) FBD of 2 to 1 distribution.

Figure 2.3: Uneven load distribution can also be achieved by changing the location of the central pivot point. Figure 2.3(a) shows a 2 to 1 ratio of the load distribution. The center pivot point is one-third distance from the left manipulator.

2.4 Passive Joints for Position Deviations

This work presents a whiffletree design that is optimized for cooperative robot manipulation. Passive joints enable positional displacements during dual-arm manipulation. This enables the two arms to move independently as as long as the relative distance between them remains fixed. Note that the relative orientation of the end-effectors can be unconstrained for modest angles (the passive joints have limited range of motion). These passive joints, each with 3 degrees of freedom, act as pivot points for the linkage that connects the two manipulators.

Figure 2.4(a) illustrates the axes of rotation possible. As Figures 2.4(b) and 2.4(c) illustrate, axes x and y provide rotations in the horizontal plane. The vertical rotation is enabled by the turntable installed at the bottom of the joint and is shown in Figure 2.4(d). Figure 2.4(e) shows that four slots are installed on the I-beam linkage to enable horizontal displacements of each end-effector. These slots allow the passive joints to slide along the linkage with approximately $5mm$ of margin of error. This provides a small degree of robustness to deviations from the relative distance constraint.

2.5 Tool Changers for Autonomous Installation

The dual-arm whiffletree gripper design can be utilized in a robotic cell with multiple manipulators assigned with individual tasks. The whiffletree gripper can be installed to two individual manipulators when it is necessary to handle heavy loads that exceed the payload of a single arm. The whiffletree can then be removed when the dual-arm task is completed. The mechanical device should be easily attachable and easily detachable when desired to allow ease of transition between cooperative manipulation and individual manipulation.

Tool changers are an excellent solution for manipulators to swap out grasping devices without human interference. For the dual-arm whiffletree gripper design, two ATI QC-11 Tool Changers were integrated into the two ends of the whiffletree. This enables an au-

tonomous quick-change locking mechanism. The tool changer consists of a master plate which interfaces with the manipulator and a tool plate which is installed on the whiffletree. The usage of this device is illustrated in the accompanying video [31]. The two plates can be joined with a locking force of up to $1100N$. Individually, the suggested payload limit of each pair is approximately $16kg$. The tool changer device also features pneumatic air lines and electric modules that allow the utilization of different types of grippers. The tool changer activation is controlled using an electronically toggled pneumatic valve on the master plate. Once the whiffletree is detached, other tools can be utilized by the manipulators.

2.6 Customizable Grasping Tools

The grasping tool of the whiffletree gripper can be customized for specific applications. However, due to the nature of the whiffletree mechanism, the grasping tool must be a device that can grasp the object perpendicular to the vertical surface. Three different designs have been illustrated in this section. Figure 2.6 illustrates the pneumatic gripper design that is used for this work. Pneumatic grippers are reliable and commonly used in industrial settings to lift heavy loads. Figure 2.7 shows the electromagnetic gripper design that can be used to lift heavy ferrous materials. Figure 2.8 depicts the more common, parallel-jaw gripper installed on the center joint of the whiffletree gripper design. The electric module that is provided by the tool changers can allow the manipulators to make use of different types of grippers.

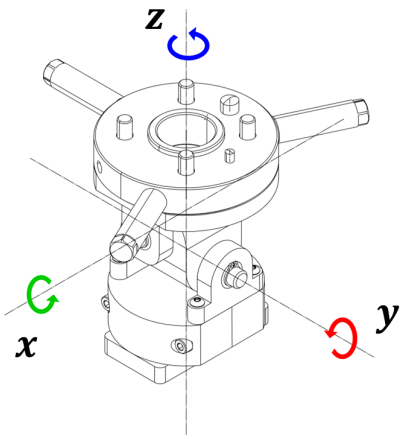

(a) Passive joint.

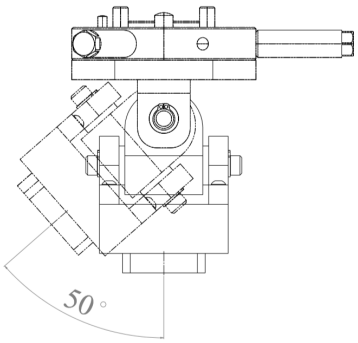

(b) Rotation about x.

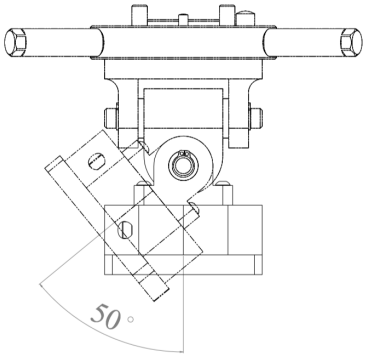

(c) Rotation about y.

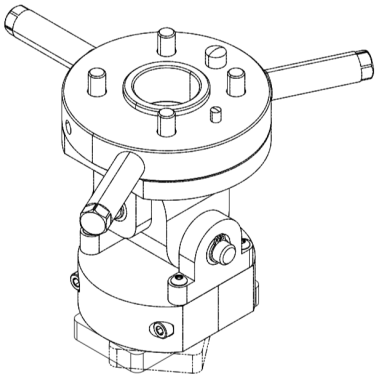

(d) Rotation about z.

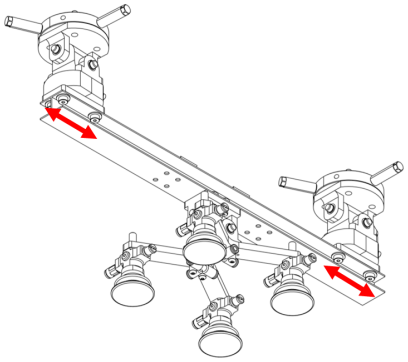

(e) Slider Mechanism.

Figure 2.4: Passive joint has 3 DOF (Figure 2.4(a)). Each degree of freedom adds an additional rotation about each principal axis (x, y, and z). Figures 2.4(b) and 2.4(c) show that the rotations about axes x and y are enabled by rotary shafts with up to 100 degrees of rotation. Figure 2.4(d) illustrates that full vertical rotation is enabled by the turntable. Slots on the I-beam linkage allow horizontal displacements from any oscillatory behavior of the manipulators (Figure 2.4(e)).

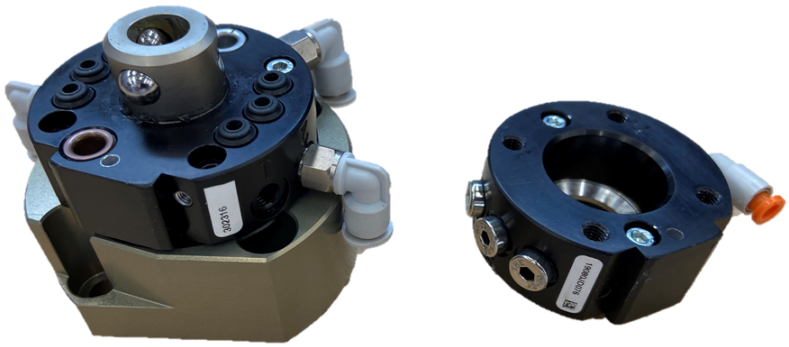

(a) Master plate (left) and tool plate (right).

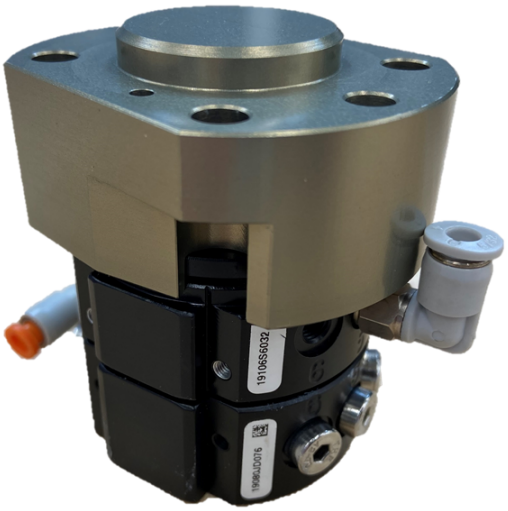

(b) Tool changers joined.

Figure 2.5: Tool changers can be implemented to allow ease of transition between different tasks. The master plate (left) and the tool plate (right) can be interfaced to join the manipulator and the gripper.

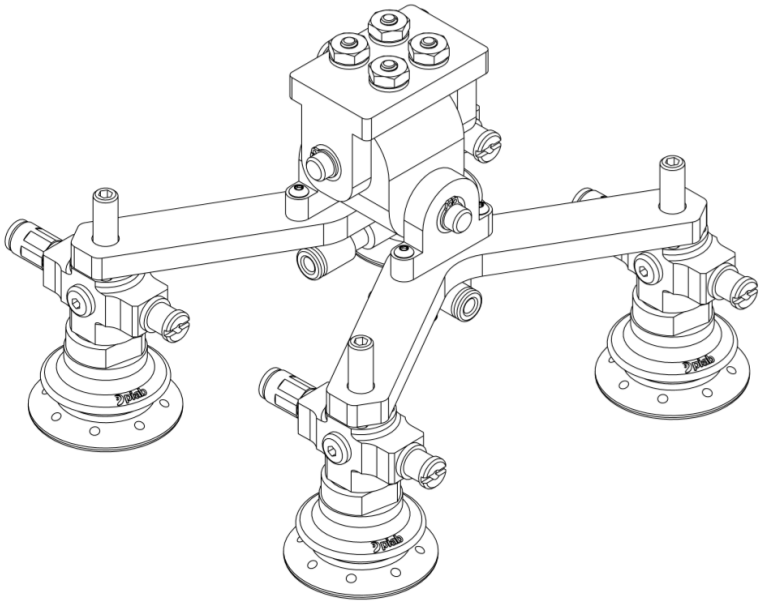

Figure 2.6: The grasping tool can be customized for desired application. For this work, pneumatic suction cups were chosen for an industrial application setting.

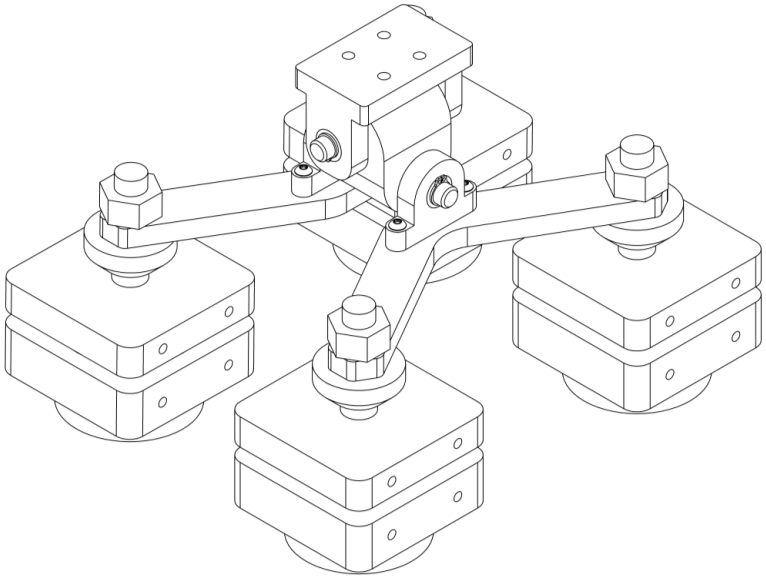

Figure 2.7: The electromagnetic gripper design can be used to lift various ferrous materials.

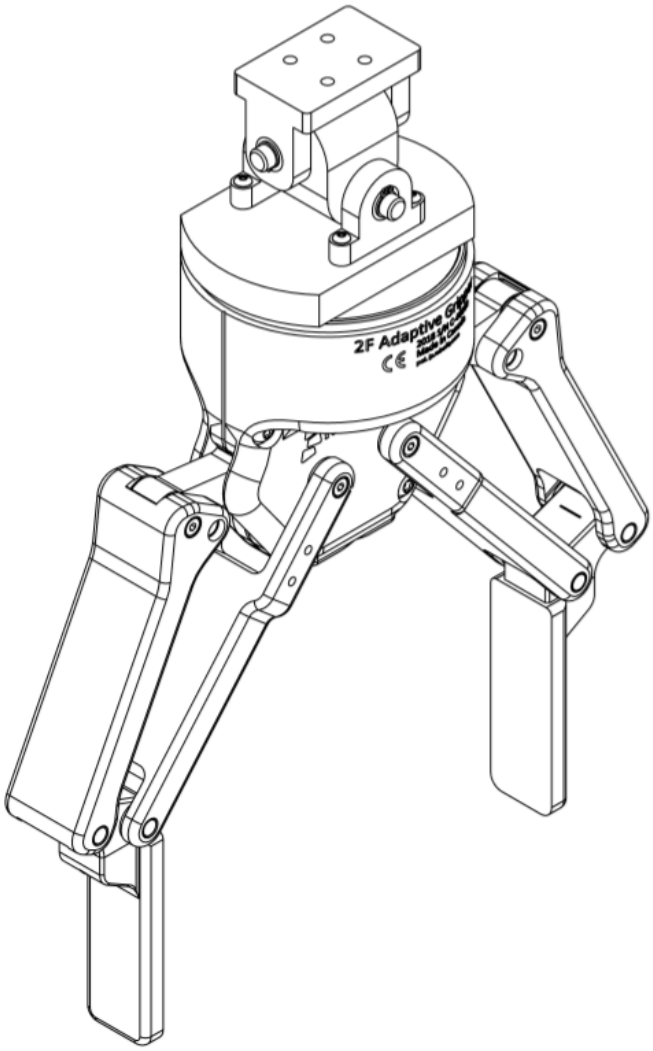

Figure 2.8: The Robotiq 2-finger parallel gripper can be installed on the center joint and controlled via the electric module on the tool changers.

CHAPTER 3

CONTROLS

3.1 Control Strategy

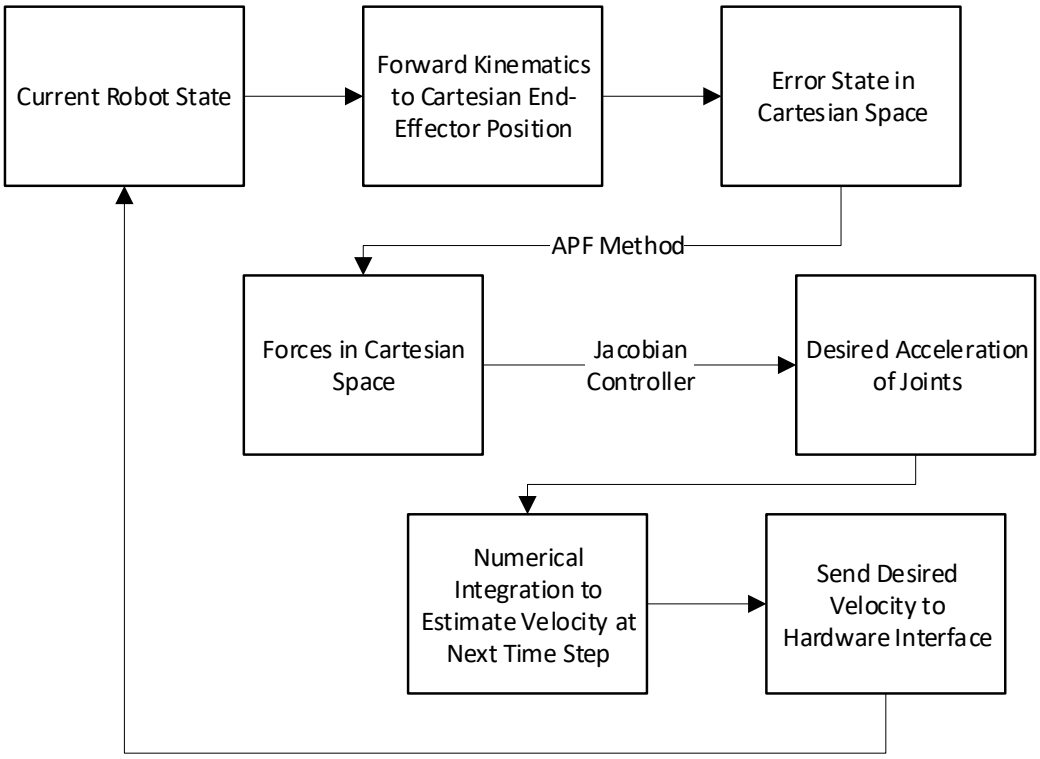

Figure 3.1: Representation of processes that occur at each time instance of control and path planning. No inverse kinematics operation is required for trajectory planning and motion.

The use of a whiffletree creates unique control challenges for the two arms. The whiffletree eliminates the need for load-balancing through control. Instead, the whiffletree physically couples the two manipulators and imposes a distance constraint on the two end-effectors. This mechanical restriction creates a need for a trajectory planner and controller that can handle 12 actuated joints with constraints in real time. To meet these requirements,

this work utilized a custom algorithm that combines a modified Artificial Potential Field (APF) trajectory planner with a Jacobian Transpose controller. The overall control strategy is outlined below:

1. A set of end-effector goal positions is defined in Cartesian space as a trajectory for the 12 DOF system.

2. A series of attractive forces is obtained by the APF method [32], using the set of desired goal positions.

3. The series of attractive forces are translated to a Jacobian Transpose controller to estimate the resulting joint accelerations of the system.

4. The joint accelerations are then numerically integrated to determine the desired joint velocities for the next time interval.

5. The resulting robot motion and the forward kinematics of the 12 DOF system are simultaneously tracked.

The APF method is designed as a series of forces that attract towards goal positions and repel against obstacles [33]. Without considering obstacles, the APF method is guaranteed to converge to a region around the goal in finite time [34]. The APF method defines constraints imposed by physical limitations and models them as goal forces with high penalties for deviation. For this work, the relative distance between the end-effectors is prioritized over the absolute position of the end-effectors in Cartesian space in order to successfully utilize the whiffletree gripper. These attractive forces applied to the end-effector can be translated to a Jacobian Transpose controller to estimate the resulting joint accelerations on the system. Numerical integration can then determine the desired joint velocities at the next time interval based on the control frequency of the system. By tracking the resulting robot motion and forward-kinematics, this information can be fed into the next control cycle for trajectory motion towards the desired goal. The control strategy is outlined in Figure 3.1.

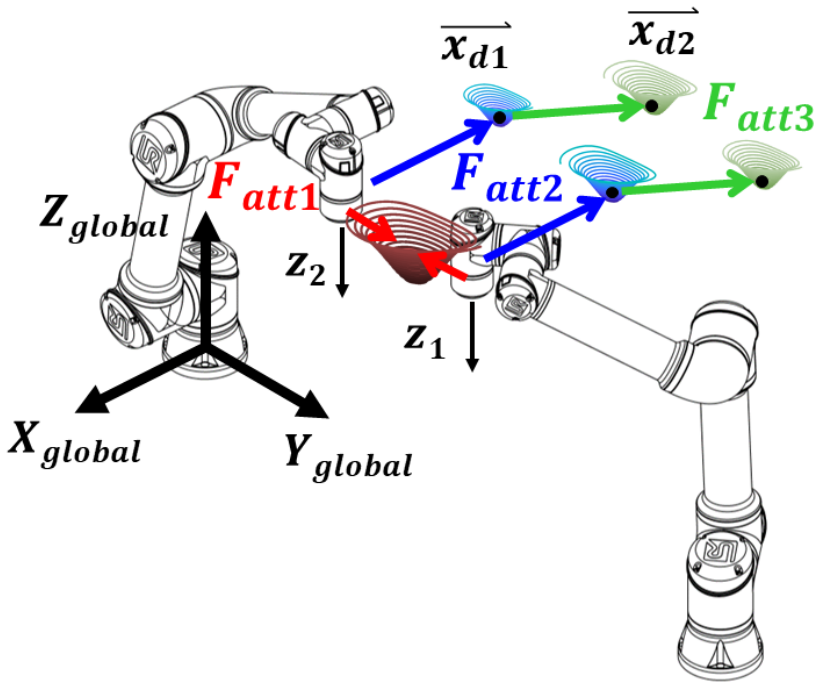

Figure 3.2: A single Cartesian coordinate frame was defined to plan the path of the two manipulators. The two end-effectors were prioritized to stay a fixed relative distance from each other using attractive forces (F_{att1}). Multiple desired goal positions were set in sequence in order to plan the path and attractive forces (F_{att2}, F_{att3}, ...) were used follow the desired trajectory.

The primary benefit of this algorithm is discarding the need for any inverse calculations. Typically, both path-planning and control algorithms for robotic manipulators require an inverse computation, since the goal states and obstacles are in Cartesian space and the controller is in joint space. Occasionally, systems will have well-defined inverse kinematics, which allow for a direct computation. However, for complex systems (such as for a 12 DOF dual-arm set up), inverse kinematics cannot be found directly and must therefore be solved numerically. However, since the APF approach does not require an inverse calculation, the computations can be performed in real time with a desktop PC. Therefore, the trajectory planner and controller can be wrapped together for each time instance instead of being separated.

The pseudo-inverse method is the most popular method for path planning with kinematically redundant systems [35]. This method, however, requires the calculation of the system's Jacobian as well as its pseudo-inverse. Furthermore, this method may have an algorithmic singularity. This creates computational complexity and failure to move towards the desired position. As a remedy, the Jacobian Transpose method was used due to its simple computation and numerically robust characteristics [36]. This method removes the problematic Jacobian inversion mentioned above. In addition, the Jacobian Transpose controller can relate an error state to joint accelerations [37]. Note the use of joint accelerations rather than the more commonly used joint velocities. The stability of this approach is proven in [37]. The form of the relationship is shown in Equation 3.1 with γ as a positive constant chosen for stability. For the equations in this section, $\vec{x}$ is described as the generalized 6 vector coordinate representing position and orientation in Cartesian space, and $\vec{x}_d$ is a desired pose.

$$\ddot{\vec{\theta}} = \gamma J^T(\vec{x}_d - \vec{x}) \tag{3.1}$$

The APF method can have convergence issues when the environment has many obstacles. However, since obstacles are not considered, the typical problems of convergence for APF methods are no longer an issue. With only goal states considered, the gradient of the potential field ($\frac{d\Psi}{d\vec{x}}$) is shown in Eq. 3.2 with k as a proportional gain of the function. To plan a motion, multiple goal states are considered, where constraints are evaluated as rigid goals. Figure 3.2 illustrates how multiple goal states were used to plan a desired trajectory of motion.

$$\frac{d\Psi}{d\vec{x}} = -k(\vec{x}_d - \vec{x}) \tag{3.2}$$

With the joint acceleration term from Eq. 3.1, the control law can be adapted to operate with the APF forces shown in Eq. 3.2. This work will mirror the efforts shown in [38], but

with the control input now in the joint domain. The result of these control laws is combined into the expression shown in Eq. 3.3, where k_v is a positive damping constant and β is the combined gain.

$$\ddot{\vec{\theta}} = -k_v \dot{\vec{\theta}} + \beta J^T \frac{d\Psi}{d\vec{x}} \tag{3.3}$$

The equations so far have demonstrated how the joint trajectory for a single arm can be calculated and executed. However, for this dual-arm manipulation task, both arms must be controlled simultaneously while maintaining a fixed distance between end-effectors. This is equivalent of having two desired locations for each manipulator. First, the arms must maintain a nominal distance between the end-effectors (within a known tolerance), and second, the arms must eventually bring the end-effectors to a desired location. The first of these desired locations is a transient relation between the arms which ensures that the whiffletree can be held by the system. This first error value is also more important than the final desired location, as the constraint in the relationship between the end-effectors must be maintained. This is achieved by having two separate attractive forces per arm that ensure the two end-effectors stay at an allowable distance to one another while converging to a desired location. For example, if one of the goal states in Cartesian space did not meet the desired distance between the end-effectors, the system would never be able to converge. These goal states can be accounted for by summing the desired positions in Eq. 3.2. The resulting system of equations is shown in Eq. 3.4. In these equations, the subscripts of 1 and 2 represent the first and second arm spaces respectively.

$$\begin{aligned} \ddot{\vec{\theta}}_1 &= -k_{v1} \dot{\vec{\theta}}_1 + \beta_1 J_1^T \frac{d\Psi_1}{d\vec{x_1}} \\ \ddot{\vec{\theta}}_2 &= -k_{v2} \dot{\vec{\theta}}_2 + \beta_2 J_2^T \frac{d\Psi_2}{d\vec{x_2}} \end{aligned} \tag{3.4}$$

This APF method is a computationally efficient approach for the kinematic control of

complex high-DOF systems. It enables tailored potential fields for the various kinematic constraints, and does not require a trajectory to be explicitly defined. These properties are desirable, but the APF method does not explicitly balance the vertical loads. The whiffletree takes care of load balancing. This makes APF control and whiffletree-based load balancing an ideal combination.

It is important to note that these terms are linear. Additional constraints per arm would complicate the calculation, but this approach is less complicated than having to perform any inverse calculations. These traits of the APF and Jacobian transpose method make this approach well-suited and practical for this whiffletree-based cooperative manipulation.

CHAPTER 4

PERFORMANCE QUANTIFICATION

4.1 Mechanical Prototype

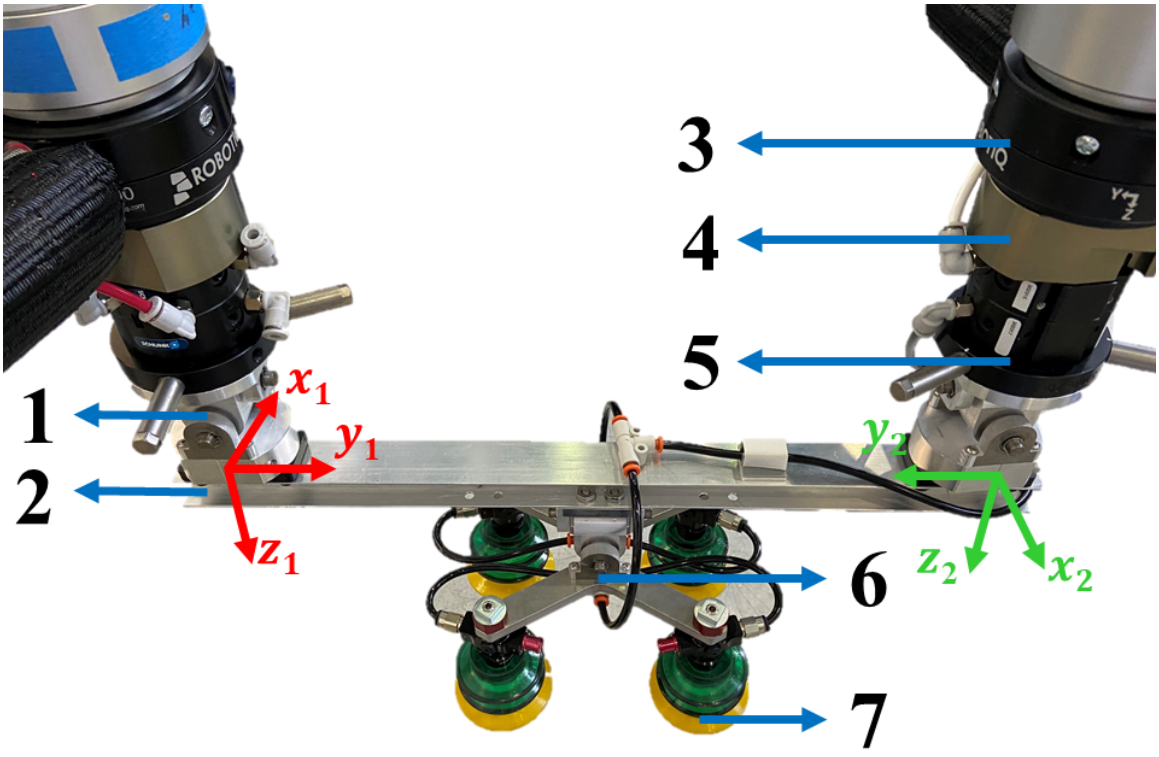

Figure 4.1: Annotated view of the fully designed and machined prototype of the dual-arm whiffletree gripper: 1) passive joint, 2) Robotiq Force-Torque Sensor, 3) Master Plate, 4) Tool Plate, 5) I-beam linkage, 6) center joint, 7) pneumatic grippers.

A physical prototype was designed, fabricated, and assembled. The two passive joints were machined out of 6061 aluminum and installed with carbon steel rotary shafts. The base of the turntable was designed and machined out of delrin and was lubricated with grease for smooth rotational motions. The I-beam linkage was machined with 6063 aluminum to approximately 13 inches in length. Slots and through-holes were machined to

allow the installation of passive joints and center joints. The center joint was also machined with 6061 aluminum and carbon steel rotary shafts. Piab VGS2010 vacuum gripper systems and four BX52P suction cups were installed on the center joint with 5/32 inch tubes. The vacuum lines were linked to a single manifold for source of air. The connections were made with push-to-connect tube fittings. The vacuum lines can be customized to link to either of the robots or both for source of air. A photo of the prototype is shown in Figure 4.1. The total mass of the entire whiffletree assembly was approximately $1kg$. When including the tool changers (master and tool plate), the total mass of the mechanical system is $2kg$.

The suction cups are each capable of holding $75N$ of force. The metal components can handle $\sim 100N$ of payload force. Each tool changer can bear $155N$ of force. The structural elements can handle $\sim 500N$ of load. Therefore, the payload of the system is limited by the suction cups. The prototype system can hold a payload of $\sim 300N$. This can be easily expanded by including more suction cups. This means this system can be easily incorporated into a range of industrial manipulators.

4.2 Experiments

Physical experiments were performed by using the dual-arm whiffletree gripper prototype in tandem with two Universal Robots UR5 manipulators. Each UR5 is capable of carrying $5kg$ payloads. The force limit is based on this rating. Since the arm trajectories keep the end effector in a constant orientation, their z-axes aligns with the earth-fixed Z-axis. The whiffletree mechanism is designed to balance loads in the whiffletree's z-axis. By keeping the end effectors flat, the whiffletree can be used to balance gravitational forces. During the experiment, the orientations of each end-effectors were set such that the z-axes align with the earth-fixed Z-axis. The experiments are illustrated in the following figures and in the accompanying video [31]. The manipulators were mounted on a steel table approximately $1.3m$ apart from each other. The robotic system is controlled using a standard PC with a Linux system and Robot Operating System (ROS).

To quantify the performance of the whiffletree gripper, the robotic system was equipped with two Robotiq FT300 Force-Torque sensors with a force range of $\pm 300N$ and torque range of $\pm 30Nm$. Each force torque sensor has a mass of $300g$, and the fastest communication rate is $100Hz$. These sensors were only used for measurement and validation, not for control.

In the experiment, the overall task is to transfer a $7kg$ box from the table to an adjacent cart. The distance that is needed to travel from the table to the cart is approximately $0.8m$. The UR5 arms are incapable of lifting the box independently and therefore must cooperate. The dual-arm manipulation process consists of three core steps:

1. In the first phase, the two UR5 manipulators approach the tool stand to install the tool changers. After installation, the manipulators approach the box and start recording force data.

2. In the second phase, the two manipulators grasp the wooden box using the pneumatic suction cups. The manipulators then lift the box and cooperatively carry it to the cart.

3. In the third phase, the suction cups are released and the box is placed on the cart. The manipulators then each return to their home positions.

This work uses the previously described control method to plan the trajectory with specific Cartesian positions. Concurrently, the end-effectors maintain a fixed distance apart from each other using the attractive forces from APF Theory. The experiment setup is shown in Figure 4.2. The dual arm manipulation task took $45s$ to complete. The complete experiment took $70s$ to finish.

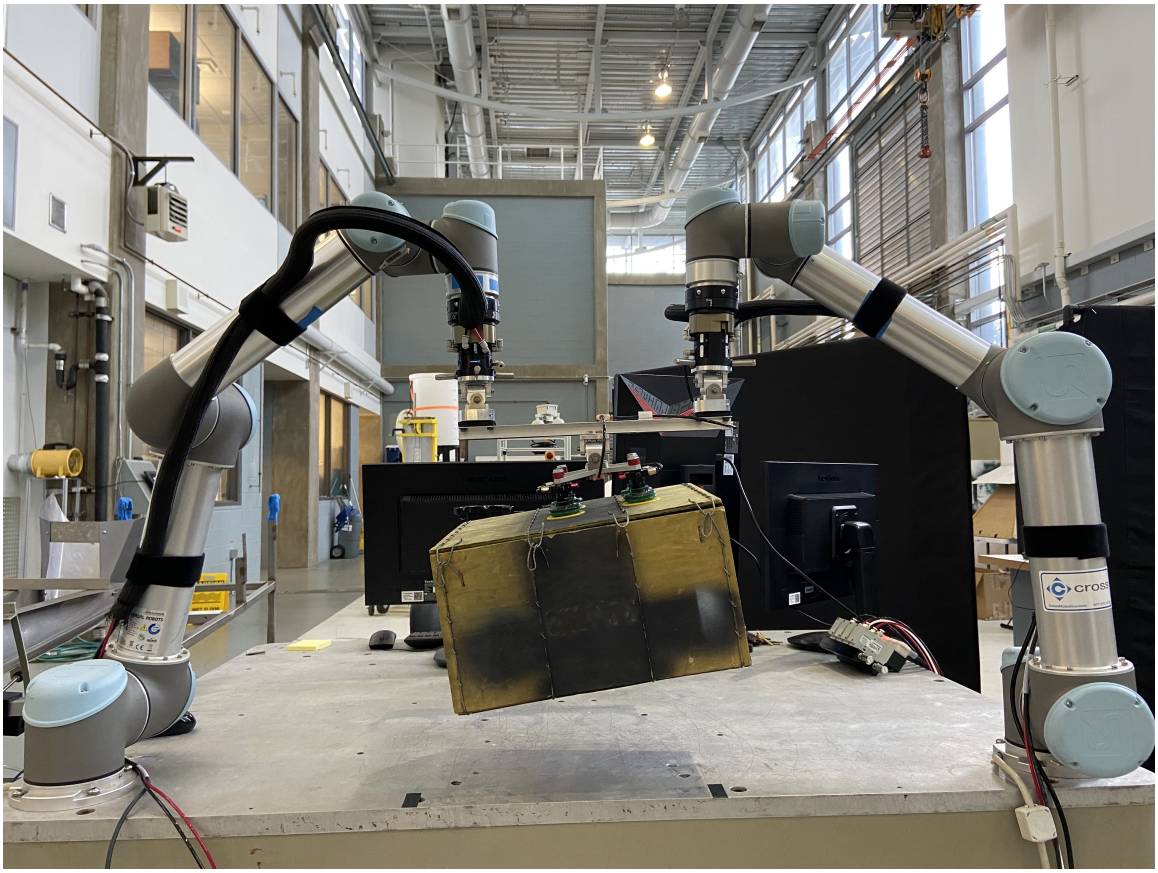

Figure 4.2: Experimental setup using two 6 DOF UR5 manipulators. The manipulators were setup $1.3m$ apart from each other to lift and carry a $7kg$ load.

Figure 4.3: Phase 1: The two UR5 manipulators approach the tool stand on the steel table to install the tool changers. The locking mechanism of the tool changers is triggered electronically via relay shield.

Figure 4.4: Phase 2: The two UR5 manipulators approach the wooden crate to grasp using the dual-arm whiffletree gripper. The plot shown on the top right indicates the force exerted on the two end-effectors in the z-direction.

Figure 4.5: Phase 2: The pneumatic suction cups are used to grasp the wooden crate and are triggered using pneumatic valves. The graph shows the force dropping initially when the suction cups are pressed down using the pneumatic suction cups.

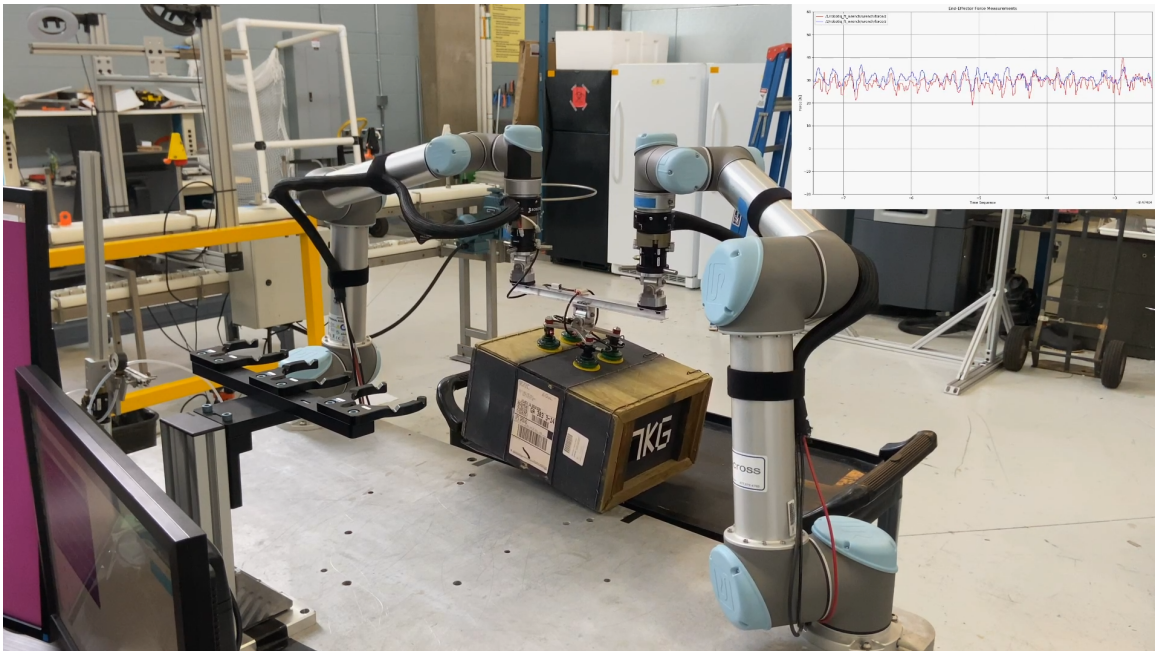

Figure 4.6: Phase 2: The two UR5 manipulators carry the box to the nearby cart. The graph shows a relatively even distribution of forces.

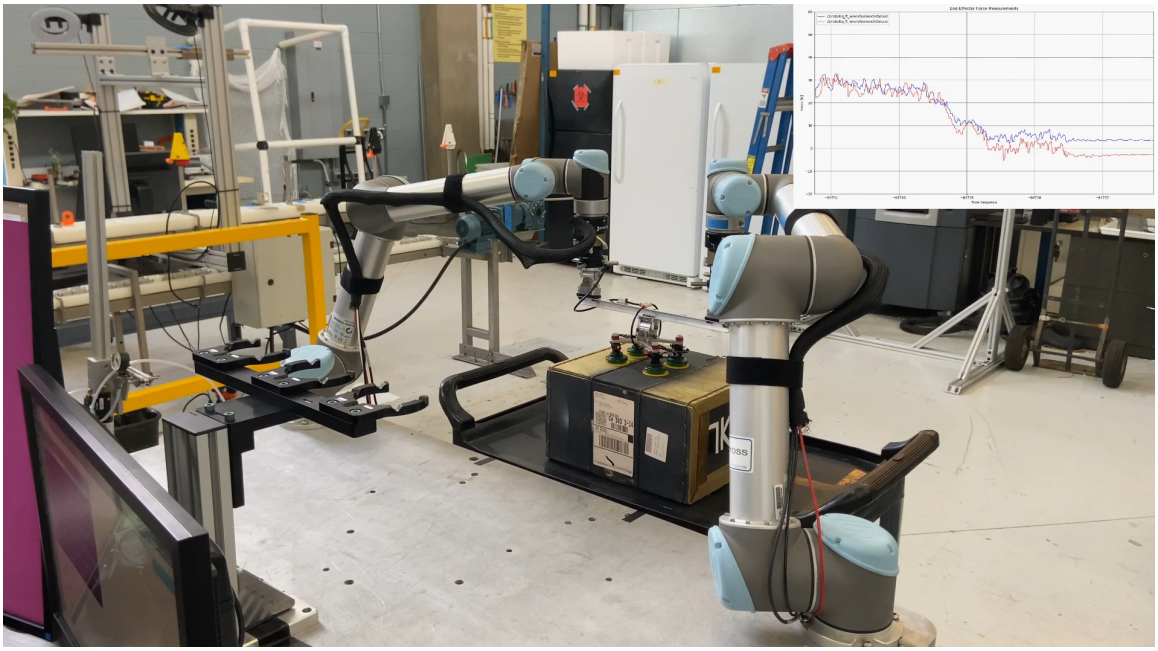

Figure 4.7: Phase 3: The box is released on the cart.

Figure 4.8: Phase 3: The two UR5 manipulators return to home position.

CHAPTER 5

RESULTS

Forces and positions from the two UR5 arms were recorded and illustrate the performance of the dual-arm manipulation strategy. The most critical consideration is ensuring that neither arm exceeded its payload limit. With the force/torque sensors attached, the z-axis load limit of each arm is estimated as $46.1N$ (due to the presence of the load cell). With a payload of $7kg$ ($68.7N$), uneven load distribution can easily exceed this amount. The end-effector forces in the z-direction on each manipulator is shown in Fig. 5.1 and 5.2. At the $17s$ mark, the manipulators grasp the box using the pneumatic suction cups. Around the $35s$ mark, the force drops as the box is placed on the desired location. This data during the lifting phase illustrates two key results. First, the force in the z-direction stays below the payload limit. Second, the force on each manipulator in the z-direction is very similar throughout the dual-arm lifting portion of the experiment. The measured z-force is $\sim 32N$ for each manipulator. This is roughly half of the total payload.

The x and y force limits of manipulators are less restrictive for the given manipulator system. Nonetheless, the x and y forces are shown in Fig. 5.3. These results illustrate that the x forces are relatively low. The y-axis forces are larger due to the rigid constraint between the two arms. However, the magnitudes are very close. This is due to the motions of the two robot arms (slow and in sync). This illustrates that effective load balancing is taking place in all directions.

The control strategy implemented in this work uses feedback from the end-effector and joint positions. The manipulator trajectories are illustrated in Fig. 5.4. These show the spatial trajectories executed by each of the end effectors.

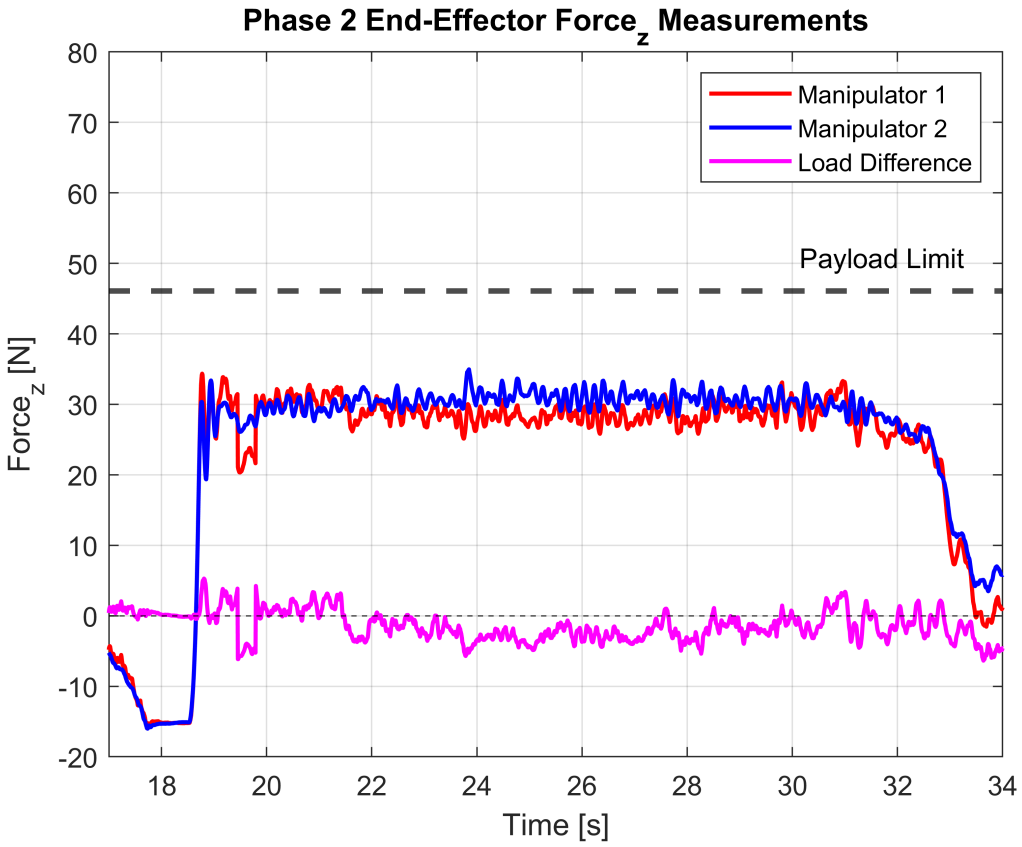

Figure 5.1: The force applied to the end-effectors in the z-direction when carrying a $7kg$ load. The forces are distributed evenly across the two manipulators.

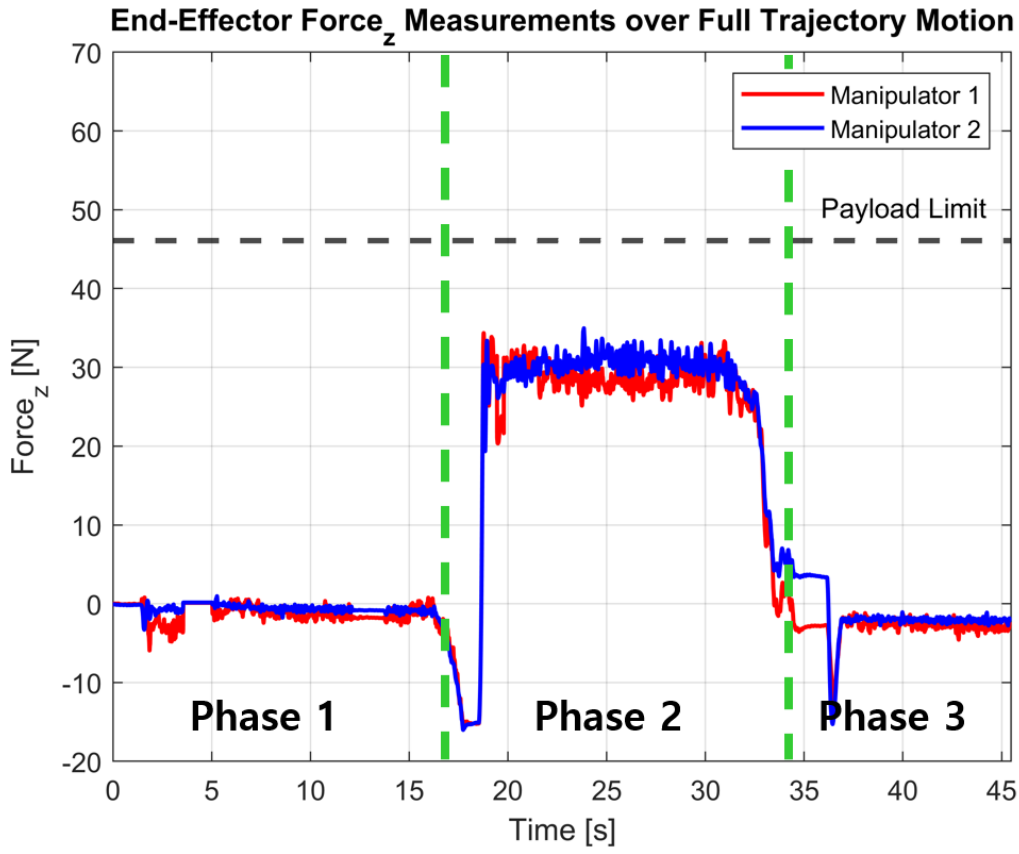

Figure 5.2: Force measurements of the two manipulators during the dual-arm manipulation task. The $17s$ mark indicate the grasping of the wooden box using pneumatic suction cups. The $35s$ mark indicate the placement of the wooden box on the cart. Note that the sensors start recording after the installation of tool changers.

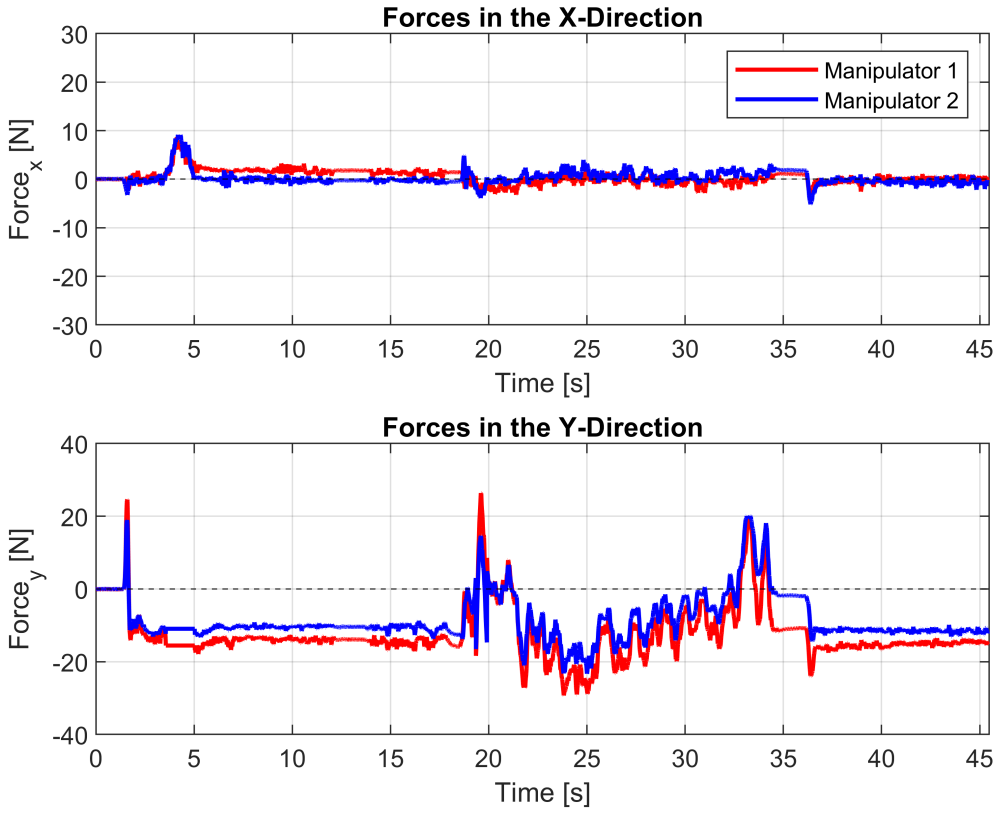

Figure 5.3: The forces applied to the end-effectors in the x and y-direction when carrying a $7kg$ load. The forces are distributed evenly across the two manipulators.

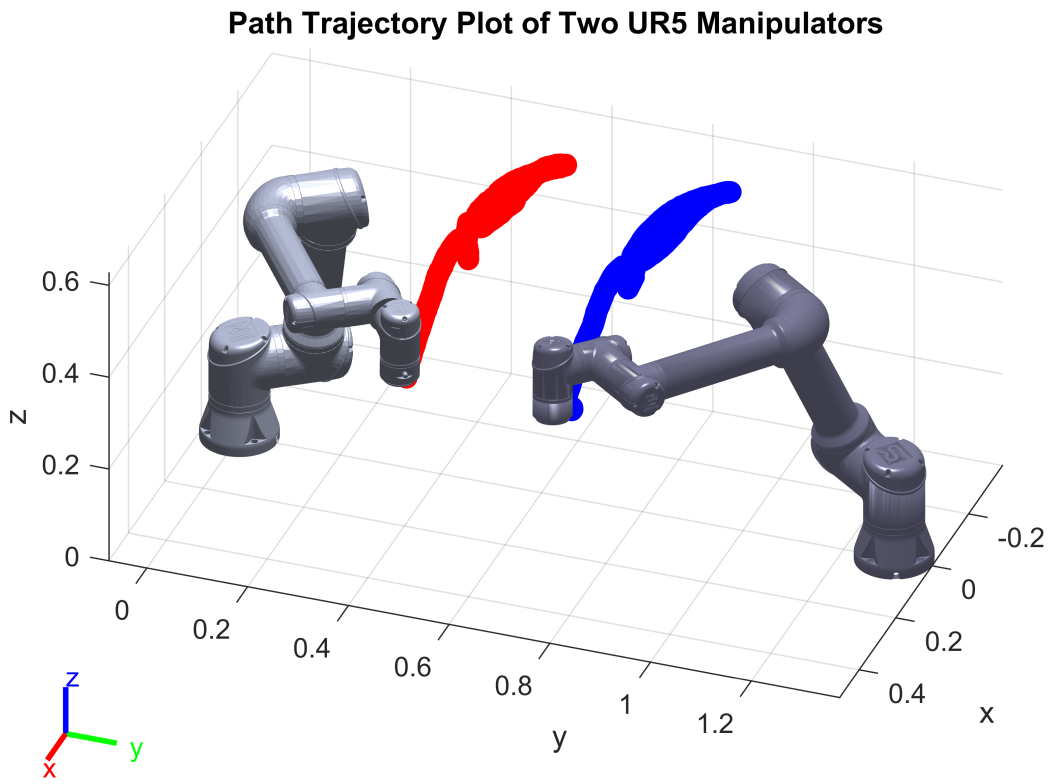

Figure 5.4: Plot of the path trajectory taken by the two UR5 manipulators during the experiment.

CHAPTER 6
CONCLUSION

This work presents a new approach for using dual-arm manipulation to move loads that exceed the capacity of a single arm. This work addresses the core challenge of load distribution by utilizing a novel whiffletree mechanism. The system can be easily adapted, uses tool changers for autonomous installation/removal, and enables the use of position-based control methods. Furthermore, this work demonstrates the performance of the described approach with a unique prototype and a full cooperative manipulation task. The experimental results demonstrate how two UR5 manipulators can move a $7kg$ load that exceeds the capacity of the individual arms. The results also illustrate that loads can be balanced with the whiffletree and kept below the failure threshold. The load balancing was achieved by leveraging the properties of the whiffletree and did not require any force sensing or feedback. The whiffletree can also be designed for autonomous customization by incorporating an adjustable gripper location. This would add weight but would enable the whiffletree to be used by a diverse set of robots (rather than only two with equal capacity).

The primary limitation with the presented approach is the limited workspace. Since the end-effectors must maintain a fixed distance from each other, the total workspace is much smaller than the workspace of an individual manipulator. However, this limitation exists for any cooperative strategy that relies on manipulating rigid bodies. Therefore, many existing cooperative manipulation methods suffer from the same drawback. This methodology holds particular promise for mobile manipulators. Such systems can utilize their moving base to greatly expand the potential workspace.

Despite this limitation, this work provides new methods and data for cooperative manipulation. The ability to handle larger payloads without resorting to a larger robot system is relevant to many applications. The approach described in this work can be utilized by

robots autonomously, and can enable existing robot cells to increase their payload capacity with minimal hardware and software modifications.

Appendices

APPENDIX A

TOOL CHANGER CONTROL

The program used to control the tool changers is given below. It was written in the Arduino environment utilizing an Arduino Uno development board using an 8-bit, AVR, 5V/16MHz atmega328p microcontroller. On the board, a 5V 4-channel relay shield is installed. Two channels are used to control each arm's tool changer, and one channel is used to control the vacuum gripper. The last channel is left unused. The board setup is shown in Figure A.1. The different channels on the board is then called using a service node in ROS.

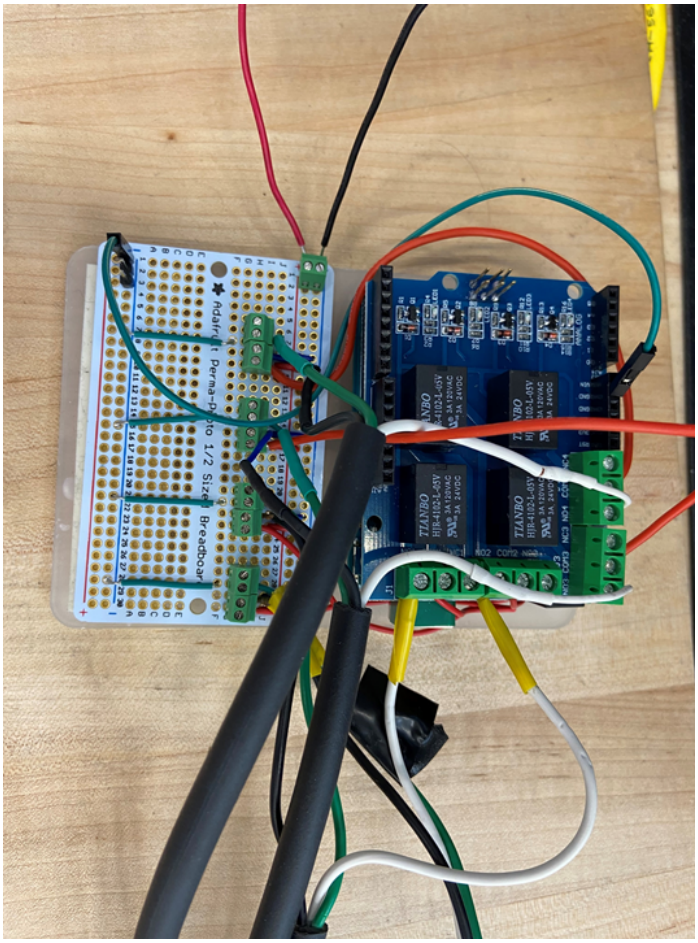

Figure A.1: The setup for the 4-channel relay shield with an Arduino Uno.

```
/**
 * This file is a short example of native arduino control over a 4 relay shield.
 *
 * Serial data performance is inconsistent
 **/

// Track relay pins and states
unsigned char relayPin[4] = {4,5,6,7};
bool relay_state[4] = {0};

// Set pinmodes and serial baud
void setup() {
    Serial.begin(9600);

    int i;
    for(i = 0; i < 4; i++) {
        pinMode(relayPin[i], OUTPUT);
    }
}

// Listen for commands and toggle individual relays
void loop() {
    while (Serial.available() > 0) {
        int input = Serial.parseInt();
        digitalWrite(relayPin[input / 10 - 1], (input % 10 == 1) ? HIGH : LOW);
    }
}
```

APPENDIX B

PNEUMATICS FOR GRASPING SYSTEM

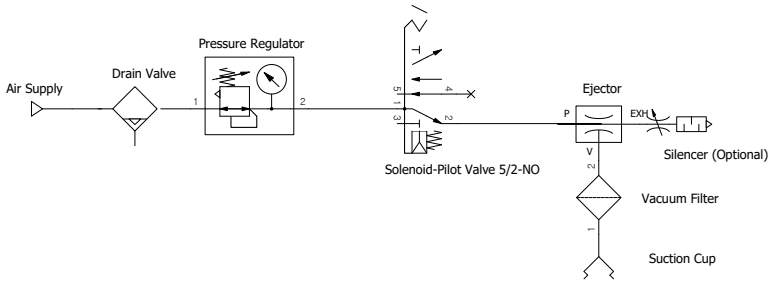

Figure B.1: Pneumatics diagram for the vacuum gripper.

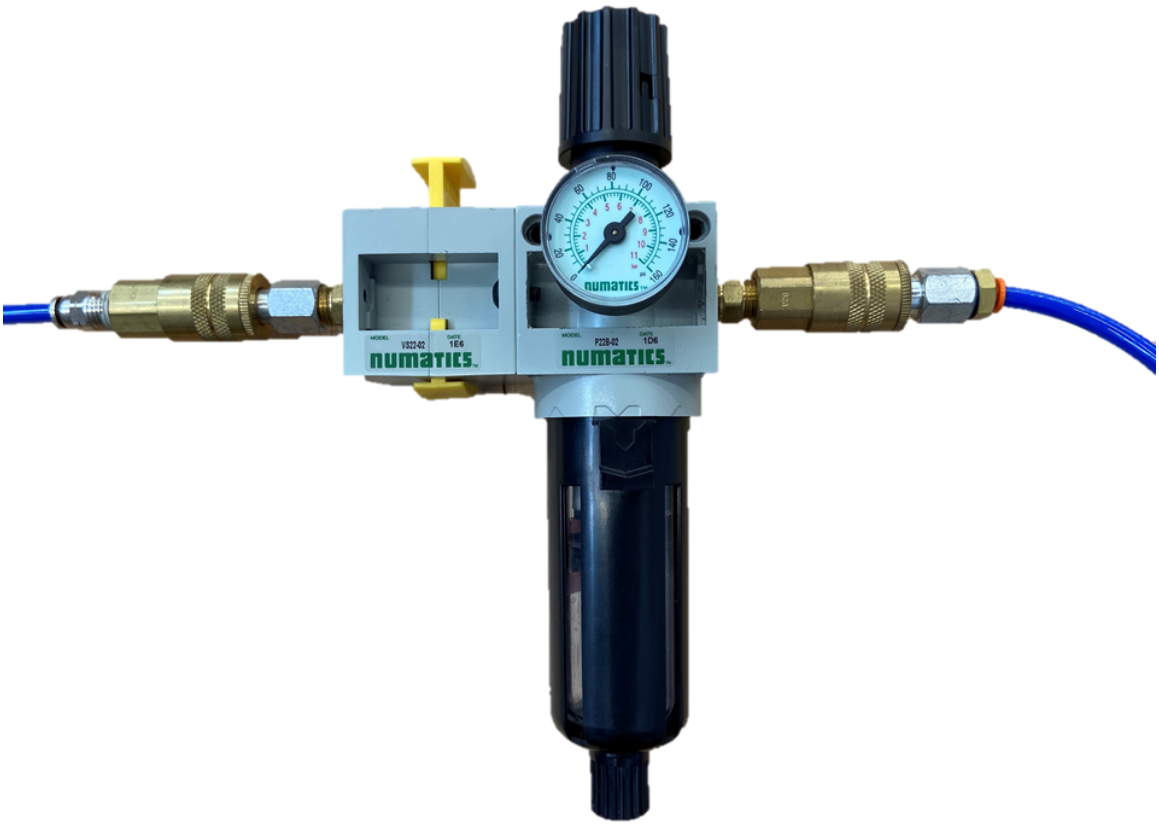

Figure B.2: Numatics Air Particulate Regulator was used to control the pressure of compressed air.

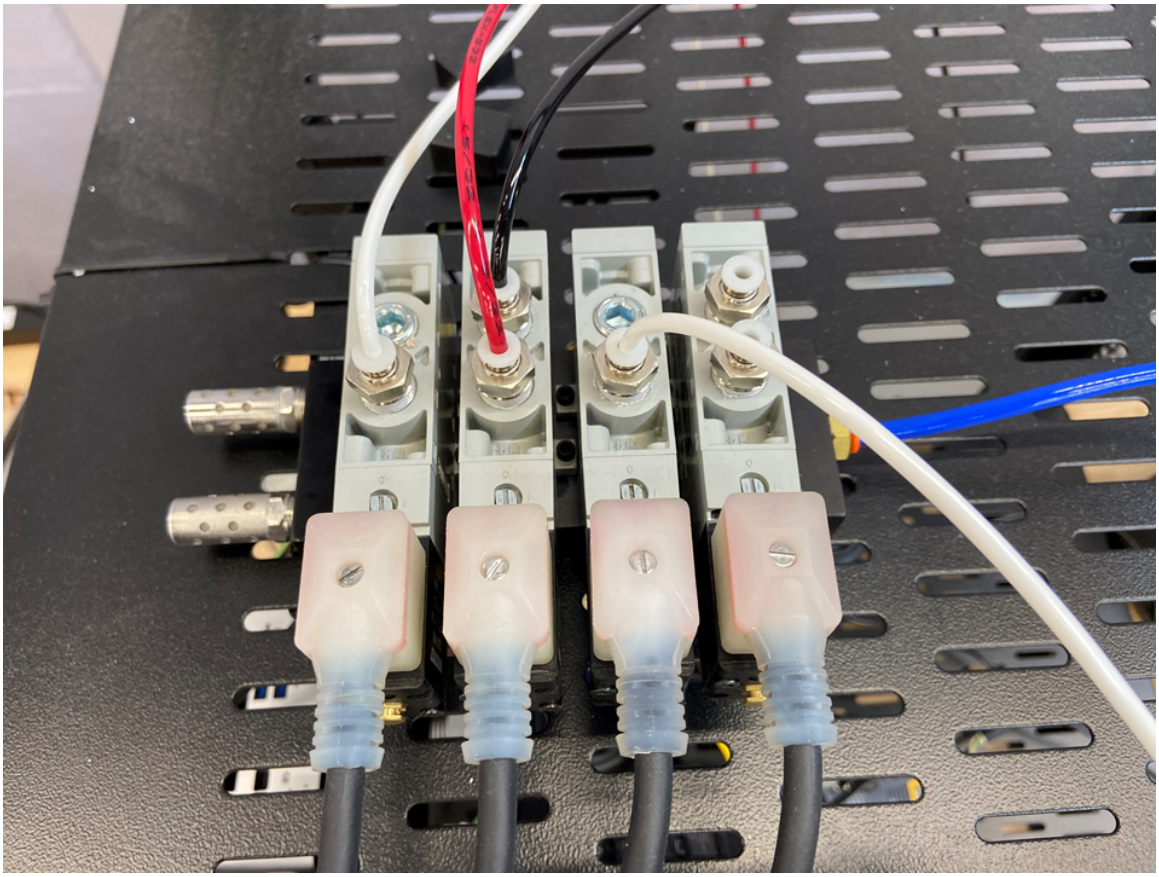

Figure B.3: Three solenoid valves were connected to the relay shield to control the tool changers and the vacuum gripper.

REFERENCES

[1] Aaron Edsinger and Charles C Kemp. "Manipulation in human environments". In: *2006 6th IEEE-RAS International Conference on Humanoid Robots*. IEEE. 2006, pp. 102–109.

[2] Daniel Kruse, Richard J Radke, and John T Wen. "Collaborative human-robot manipulation of highly deformable materials". In: *2015 IEEE international conference on robotics and automation (ICRA)*. IEEE. 2015, pp. 3782–3787.

[3] Bruno Vilhena Adorno. "Two-arm manipulation: From manipulators to enhanced human-robot collaboration". PhD thesis. 2011.

[4] YF Zheng and JYS Luh. "Control of two coordinated robots in motion". In: *1985 24th IEEE Conference on Decision and Control*. IEEE. 1985, pp. 1761–1766.

[5] Y Zheng and J Luh. "Joint torques for control of two coordinated moving robots". In: *Proceedings. 1986 IEEE International Conference on Robotics and Automation*. Vol. 3. IEEE. 1986, pp. 1375–1380.

[6] II Kab and Yuan F Zheng. "Unknown load distribution of two industrial robots". In: (1991).

[7] Lei Yan et al. "Coordinated compliance control of dual-arm robot for payload manipulation: Master-slave and shared force control". In: *2016 IEEE/RSJ International Conference on Intelligent Robots and Systems (IROS)*. IEEE. 2016, pp. 2697–2702.

[8] Michael A Unseren and Antti J Koivo. "Reduced order model and decoupled control architecture for two manipulators holding an object". In: *Proceedings, 1989 International Conference on Robotics and Automation*. IEEE. 1989, pp. 1240–1245.

[9] Vijay Kumar et al. "Control of contact conditions for manipulation with multiple robotic systems". In: *Proceedings. 1991 IEEE International Conference on Robotics and Automation*. IEEE. 1991, pp. 170–175.

[10] Samad Hayati. "Hybrid position/force control of multi-arm cooperating robots". In: *Proceedings. 1986 IEEE International Conference on Robotics and Automation*. Vol. 3. IEEE. 1986, pp. 82–89.

[11] Masaru Uchiyama and Pierre Dauchez. "A symmetric hybrid position/force control scheme for the coordination of two robots". In: *Proceedings. 1988 IEEE International Conference on Robotics and Automation*. IEEE. 1988, pp. 350–356.

[12] Xiaoping Yun. “Nonlinear feedback control of two manipulators in presence of environmental constraints”. In: *Proceedings, 1989 International Conference on Robotics and Automation*. IEEE. 1989, pp. 1252–1257.

[13] Carl D Kopf and Tetsuro Yabuta. “Experimental comparison of master/slave and hybrid two arm position/force control”. In: *Proceedings. 1988 IEEE International Conference on Robotics and Automation*. IEEE. 1988, pp. 1633–1637.

[14] Yun-Hui Liu, Suguru Arimoto, and Tsukasa Ogasawara. “Decentralized cooperation control: non-communication object handling”. In: *Proceedings of IEEE International Conference on Robotics and Automation*. Vol. 3. IEEE. 1996, pp. 2414–2419.

[15] T Tarn, A Bejczy, and Xiaoping Yun. “Coordinated control of two robot arms”. In: *Proceedings. 1986 IEEE International Conference on Robotics and Automation*. Vol. 3. IEEE. 1986, pp. 1193–1202.

[16] John T Wen and Kenneth Kreutz-Delgado. “Motion and force control of multiple robotic manipulators”. In: *Automatica* 28.4 (1992), pp. 729–743.

[17] Kazuhiro Kosuge et al. “Decentralized control of robots for dynamic coordination”. In: *Proceedings 1995 IEEE/RSJ International Conference on Intelligent Robots and Systems. Human Robot Interaction and Cooperative Robots*. Vol. 1. IEEE. 1995, pp. 76–81.

[18] Ping Hsu. “Control of multimanipulator systems-trajectory tracking, load distribution, internal force control, and decentralized architecture”. In: *Proceedings, 1989 International Conference on Robotics and Automation*. IEEE. 1989, pp. 1234–1239.

[19] Ning Xi, Tzyh-Jong Tarn, and Antal K Bejczy. “Intelligent planning and control for multirobot coordination: An event-based approach”. In: *IEEE transactions on robotics and automation* 12.3 (1996), pp. 439–452.

[20] Dong Sun and James K Mills. “Manipulating rigid payloads with multiple robots using compliant grippers”. In: *IEEE/ASME transactions on mechatronics* 7.1 (2002), pp. 23–34.

[21] Jing Zhang et al. “Sharing inertia load between multiple robots with active compliant grippers using trajectory pre-shaping”. In: *IEEE International Conference on Robotics and Automation, 2004. Proceedings. ICRA’04. 2004*. Vol. 3. IEEE. 2004, pp. 2574–2581.

[22] Suguru Arimoto, Fumio Miyazaki, and Sadao Kawamura. “Cooperative motion control of multiple robot arms or fingers”. In: *Proceedings. 1987 IEEE International Conference on Robotics and Automation*. Vol. 4. IEEE. 1987, pp. 1407–1412.

[23] Hisashi Osumi and Tamio Arai. “Cooperative control between two position-controlled manipulators”. In: *Proceedings of the 1994 IEEE International Conference on Robotics and Automation*. IEEE. 1994, pp. 1509–1514.

[24] Jakob de Nachtegaal. *Hoisting Yoke*. U.S. Patent 4,394,041. 1983, July 19.

[25] Ruediger Maximilian Seyff. *Three-crane lifting beam*. U.S. Patent 3,513,987. 1970, May 26.

[26] Eduard Meisinger and Herbert Steiner. *Hoisting gear on the trolley of a container crane*. U.S. Patent 5,314,262. 1994, May 24.

[27] Charles Anderson. *Animal Lift Frame*. U.S. Patent 4,831,967. 1989, May 23.

[28] Kai Xu et al. “Wrist-powered partial hand prosthesis using a continuum whiffle tree mechanism: A case study”. In: *IEEE Transactions on Neural Systems and Rehabilitation Engineering* 26.3 (2018), pp. 609–618.

[29] Joshua Paquette, Jeroen Van Dam, and Scott Hughes. “Structural testing of 9m carbon fiber wind turbine research blades”. In: *45th AIAA Aerospace Sciences Meeting and Exhibit*. 2007, p. 816.

[30] Wilson Ruotolo, Frances S Roig, and Mark R Cutkosky. “Load-Sharing in Soft and Spiny Paws for a Large Climbing Robot”. In: *IEEE Robotics and Automation Letters* 4.2 (2019), pp. 1439–1446.

[31] Raymond Kim et al. *Enhancing Payload Capacity with Dual-Arm Manipulation and Reconfigurable Mechanical Intelligence*. `http://youtu.be/PxlWbcDmUJg`. Accessed: 2020/06/16.

[32] J. Barraquand, B. Langlois, and J. . Latombe. “Numerical potential field techniques for robot path planning”. In: *IEEE Transactions on Systems, Man, and Cybernetics* 22.2 (1992), pp. 224–241.

[33] Oussama Khatib. “Real-time obstacle avoidance for manipulators and mobile robots”. In: *Autonomous robot vehicles*. Springer, 1986, pp. 396–404.

[34] Yoram Koren, Johann Borenstein, et al. “Potential field methods and their inherent limitations for mobile robot navigation.” In: *ICRA*. Vol. 2. 1991, pp. 1398–1404.

[35] Alain Liegeois et al. “Automatic supervisory control of the configuration and behavior of multibody mechanisms”. In: *IEEE transactions on systems, man, and cybernetics* 7.12 (1977), pp. 868–871.

[36] Samuel R Buss. “Introduction to inverse kinematics with jacobian transpose, pseudoinverse and damped least squares methods”. In: *IEEE Journal of Robotics and Automation* 17.1-19 (2004), p. 16.

[37] Zoran R Novakovic and Bojan Nemec. “A solution of the inverse kinematics problem using the sliding mode”. In: *IEEE Transactions on Robotics and Automation* 6.2 (1990), pp. 247–252.

[38] Konrad J Ahlin, Nader Sadegh, and Ai-Ping Hu. “The Secant Method: Global Trajectory Planning With Variable Radius, Solid Obstacles”. In: *Dynamic Systems and Control Conference*. Vol. 51913. American Society of Mechanical Engineers. 2018, V003T32A015.